İSTANBUL UNIVERSITY CERRAHPAŞA

RESEARCH ARTICLE

Electrica 2020; 20(1): 28-40

MRAS-Based Speed and Parameter Estimation for a Vector-Controlled PMSM Drive

Sai Shiva Badini, Vimlesh Verma

Department of Electrical Engineering, National Institute of Technology Patna, India

Cite this article as: Badini, SS, Verma Vimlesh. MRAS-Based Speed and Parameter Estimation for a Vector-Controlled PMSM Drive. *Electrica*, 2020; 20(1): 28-40.

ABSTRACT

This paper presents the estimation techniques for rotor speed (ω_r), rotor position (ρ_{mr}), and stator resistance (R_s) for a Permanent-Magnet Synchronous-Motor (PMSM) drive. An online speed-/position- estimation technique is essential to make the drive mechanically robust and to increase its reliability. The instantaneous and steady state Fictitious Quantity (Y) is used to build a Model Reference Adaptive System (MRAS) as a basic structure for estimating ω_r and R_s for a vector-controlled PMSM drive. MRAS models are constructed using reference voltages and actual currents in a rotor reference frame. This scheme involves less computation effort and simple expressions without any integration and differentiation terms. The Y-MRAS speed-estimation technique performs satisfactorily over a reactive power MRAS-based speed estimator under a slow zero crossing for the PMSM drive. However, this technique depends on stator resistance. The proper identification of R_s (by YR-MRAS) gives information about the machine's operating range and is also used in the online R_s compensation for the Y-MRAS technique. The proposed methods are applicable to all types of PMSM machines and are verified for various speed and load variations. The viability and effectiveness of the ω_r and R_s estimation techniques are demonstrated via stability/sensitivity analyses, MATLAB software simulations, and Typhoon Hardware In-the-Loop (HIL) - 402.

Keywords: Condition monitoring, speed control, PMSM, sensorless, stator-resistance estimation

Introduction

The Permanent-Magnet Synchronous-Motor (PMSM) drive has been in demand over the past few decades, particularly in the context of robots, electric vehicles, and industry. This is due to its efficiency, large torque/volume ratio, consistent operation, and simple structure. The presence of a permanent magnet in the rotor gives the drive an advantage over induction machines and wound rotor-type synchronous machines. The rotor position (p_{mr}) is essential for the sensorless speed PMSM drive. The mechanical, electronic speed, and position sensors make the drive expensive and reduce its reliability. When considering signal transmission and environmental issues, sensorless operation is preferable. From all the control techniques available in the literature, the dynamic performance of the vector-controlled drive gives it a significant advantage over other control techniques [1-2].

Many techniques for sensorless speed are presented in the available literature on PMSM drives [2-11]. These are mainly classified into model-based techniques [6, 12, 13] that are based on back EMF [14, 15], signal injection (SI) [4, 16], and state observer [5, 17-19] approaches along with others like artificial intelligence [7, 20-22]. Back EMF-based estimation techniques use back EMF (e) to estimate the rotor speed; this approach performs satisfactorily at high and moderate speeds. However, under zero or low-speed operation, e becomes negligible and cannot be tracked. This makes estimating the speed very difficult in addition to the sensitivity to machine parameters. The SI-based technique estimates speed based on the saliency of the machine and is the only technique that performs with high accuracy at zero speed. Nonetheless, it requires external hardware for high-frequency SI and to extract the position. A combination of e- and SI-based methods is superior to all techniques with the advantages of high- and low-speed operation, respectively; unfortunately, this scheme is too expensive.

Corresponding Author:
Sai Shiva Badini

E-mail:
badinisai.eepg16@nitp.ac.in

Received: 04.11.2019

Accepted: 06.12.2019

DOI: 10.5152/electrica.2020.19039

Observer-based approaches (such as the extended Luenburger observer, the Kalman filter, and the sliding model) are more sensitive both to machine parameters and greater complexity. The primary advantage of observer methods is that they treat the parameters as state variables and can be estimated along with the shaft speed. However, Kalman filter require initial conditions, e- and SI-based method requires filters, these degrades their advantages.

The MRAS computes functional candidates that are expressed in different forms in equal quantities and which are used in adjustable and reference models [6, 8, 23, 24]. The reference model is independent of the unknown quantity (i.e., speed), while the adjustable model is unknown-quantity dependent. The difference between these two quantities results in errors, which are passed through the PI controller (the adaption mechanism). The PI output (i.e., speed) is used to tune the adjustable model; this continues until the error is zero. These MRAS-based techniques are advantageous in terms of stability, simplicity, and reduced computational complexity. They require no extra hardware, they are free from integrator and differentiation terms, and they are also less dependent on machine parameters. Alternative techniques, such as artificial intelligence [25-27] (ANN, fuzzy logic, etc.) are recent approaches; however, they require huge memory capacities to train the system and are more complex to build.

The Q-MRAS [6] speed-estimation technique is problematic in the context of zero crossing, which is overcome using the þ-MRAS [8] and the proposed Y-MRAS techniques [28]. The proposed fictitious quantity (Y) Y-MRAS method depends on both stator resistance and mutual flux linkage ($\lambda_{\alpha f}$), although $\lambda_{\alpha f}$ varies with the aging of magnets. The fluctuates with the temperature of a machine's stator winding. This deteriorates the performance of the proposed scheme at low speeds. At high speeds, the vector control fails ($i_{ds} \neq 0$, the *d*-axis current in the rotor reference frame), although machines tend to rotate at the reference speed (ω_{ref}). The accurate speed/position estimation is achieved by precise stator resistance; therefore, online estimation techniques for compensation are required [8, 12, 29-37].

This paper proposes a new YR-MRAS stator-resistance-estimation technique for the PMSM drive. The machine temperature and operating range can be monitored using a YR-MRAS approach. The presented stability/sensitivity analyses use MATLAB simulation results and validation in real-time Typhoon hardware in-the-loop (HIL) (Typhoon-HIL, Zurich, Switzerland, EUROPE) [38] to highlight the performance of the proposed algorithms.

Section II presents the PMSM modeling. Section III presents the proposed Y-MRAS-based rotor-speed-estimation technique for a vector-controlled PMSM drive. Section IV performs stability and sensitivity analyses with respect to stator resistance for the proposed speed-estimation technique. The YR-MRAS stator-resistance-estimation technique is introduced in Section V. Sections VI and VII present the simulation and real-time HIL results for the proposed techniques before concluding in Section VIII.

PMSM Modeling

The PMSM machine modeling is taken from [2]. In the rotor reference frame, the *d*- and *q*-axes stator voltages (v_{ds} and v_{qs}) of the PMSM are expressed in the stator currents (i_{ds} and i_{qs}) in Eq.1:

$$\begin{pmatrix} v_{ds} \\ v_{qs} \end{pmatrix} = \begin{bmatrix} R_s + L_d p & -\omega_s L_q \\ \omega_s L_d & R_s + L_q p \end{bmatrix} \begin{pmatrix} i_{ds} \\ i_{qs} \end{pmatrix} + \begin{pmatrix} 0 \\ \omega_s \lambda_{af} \end{pmatrix} \quad (1)$$

$$T_e = \left(\frac{3}{2}\right) P\{i_{qs}\lambda_{af} + (L_d - L_q) i_{ds} i_{qs}\} \quad (2)$$

$$T_e - T_L = J\frac{d\omega_r}{dt} + B\omega_r \quad (3)$$

Equation 2 shows the electrical torque (T_e) developed, and Eq. 3 demonstrates the electromechanical dynamics equation. The following are definitions of the symbols and variables: T_l represents the load—torque, respectively. Pole pair (P), electrical (ω_s) and mechanical (ω_r) shaft speeds, $\omega_s = P\omega_r$ *d*-axis inductance (L_d), *q*-axis inductance (L_q), p= derivative term ($\frac{d}{dt}$), mutual flux linkage ($\lambda_{\alpha f}$), and machine inertia (J). =stator resistance, viscous coefficient (B), and electrical position (P_{ms}). The machine is the non-saliency type with a sinusoidal back EMF waveform. Table 1 contains the parameters.

The Y-MRAS-Based Speed-Estimation Technique

In the expression for the reference and adjustable MRAS models, Y is expressed as [6, 24, 39].

$$Y_1 = v_{qs}^* i_{qs} - v_{ds}^* i_{ds} \quad (4)$$

Substituting (1) in (4):

$$Y_2 = R_s\left(i_{qs}^2 - i_{ds}^2\right) + \left(L_q i_{qs}\frac{di_{qs}}{dt} - L_d i_{ds}\frac{di_{ds}}{dt}\right) + \omega_s i_{qs} i_{ds}\left(L_d + L_q\right) + \omega_s i_{qs}\lambda_{af} \quad (5)$$

Under a steady state condition, $\frac{d}{dt} = 0$, and Y_2 becomes: [31]

$$Y_3 = R_s\left(i_{qs}^2 - i_{ds}^2\right) + \omega_s i_{qs} i_{ds}\left(L_d + L_q\right) + \omega_s i_{qs}\lambda_{af} \quad (6)$$

Table 1. PMSM machine parameters [44]

Pole Pair (P)	4
Rated Speed (ω_r) (rpm)	2000
Power (KW)	1.5
Voltage (V)	254
Current (A)	3.7
Inductance Ls (mH)	22.5
Mutual Flux Linkage (λ_{af})	0.2026
Stator Resistance (R_s) (Ω)	1.6
Inertia (J) (kg-m^2)	0.0027
Viscus coefficient (B) (kg m^2/s^2)	0.34

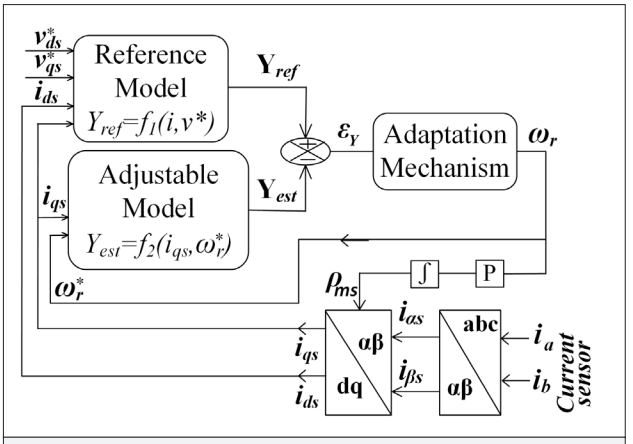

Figure 1. The Y-MRAS-based speed-estimation technique

The condition for vector control is i_{ds}=0, where Y_3 becomes:

$$Y_4 = \mathrm{R}_s i_{qs}^2 + \omega_s i_{qs} \lambda_{af} \tag{7}$$

In Eqs. 4–7, Y_2 and Y_3 are reliant on all machine parameters, and the noise is increased due to the presence of $\frac{d}{dt}$. Therefore, Y_4 and Y_1 are considered as the adjustable and the reference models, respectively, as shown in Figure 1. Y_1 is independent of shaft speed, while Y_4 is shaft-speed dependent. The error $(\text{i.e.}, \varepsilon_y = Y_1 - Y_4)$ developed in Eq. 9 is passed through a PI controller. The output (i.e., the estimated rotor speed $\omega_r^*]$ from Eq. 8 is used to tune the adjustable quantity; this continues until the error is zero. Equation 10 contains the rotor position from the speed (Figure 1).

$$\omega_r^* = k_p * \varepsilon_y + k_i * \int_0^t \varepsilon_y dt + \omega_r^*(0) \tag{8}$$

$$\varepsilon_y = (v_{qs}^* i_{qs} - v_{ds}^* i_{ds}) - (\mathrm{R}_s i_{qs}^2 + \omega_r^* P i_{qs} \lambda_{af}) \tag{9}$$

$$\rho_{ms} = \int \omega_s dt = P\rho_{mr} = P \int \omega_r dt \tag{10}$$

Stability and Sensitivity Analyses

Stability analysis

Instability under various conditions is one of the major problems with the rotor-speed-estimation technique. Here, a small-signal stability analysis [40, 41] of the Y-MRAS speed-estimation technique for the PMSM drive is performed and presented in the rotor reference frame. The state–space equations are presented in Eq. 11 for the PMSM machine (from Eq. 1 in terms of currents).

$$\begin{bmatrix} \dot{i}_{ds} \\ \dot{i}_{qs} \end{bmatrix} = \begin{bmatrix} \frac{-\mathrm{R_s}}{\mathrm{L_d}} & \frac{\omega_s \mathrm{L_q}}{\mathrm{L_d}} \\ \frac{-\omega_s \mathrm{L_d}}{\mathrm{L_q}} & \frac{-\mathrm{R_s}}{\mathrm{L_q}} \end{bmatrix} \begin{pmatrix} \mathrm{i_{ds}} \\ \mathrm{i_{qs}} \end{pmatrix} + \begin{bmatrix} \frac{1}{\mathrm{L_d}} & 0 \\ 0 & \frac{1}{\mathrm{L_q}} \end{bmatrix} \begin{pmatrix} \mathrm{v_{ds}} \\ \mathrm{v_{qs}} \end{pmatrix} + \begin{bmatrix} 0 \\ \frac{-\omega_s \lambda_{af}}{\mathrm{L_q}} \end{bmatrix} \tag{11}$$

$$\begin{pmatrix} \mathrm{i_{ds}} \\ \mathrm{i_{qs}} \end{pmatrix} = \begin{bmatrix} 1 & 0 \\ 0 & 1 \end{bmatrix} \begin{pmatrix} \mathrm{i_{ds}} \\ \mathrm{i_{qs}} \end{pmatrix} \tag{12}$$

In Eqs. 11 and 12, the state variables are the stator currents in the *d*- and *q*-axes reference frames. The general form of state–space representation is:

$$\dot{x} = Ax + Bu + E \tag{13}$$

$$y = Cx + Du \tag{14}$$

Comparing Eqs. 11–14 produces:

$$\mathrm{A} = \begin{bmatrix} \frac{-\mathrm{R_s}}{\mathrm{L_d}} & \frac{\omega_s \mathrm{L_q}}{\mathrm{L_d}} \\ \frac{-\omega_s \mathrm{L_d}}{\mathrm{L_q}} & \frac{-\mathrm{R_s}}{\mathrm{L_q}} \end{bmatrix}, \mathbf{B} = \begin{bmatrix} \frac{1}{\mathrm{L_d}} & 0 \\ 0 & \frac{1}{\mathrm{L_q}} \end{bmatrix}, \mathrm{C} = \begin{bmatrix} 1 & 0 \\ 0 & 1 \end{bmatrix}, \mathrm{D} = 0', \ \mathrm{E} = \begin{bmatrix} 0 \\ \frac{-\omega_s \lambda_{af}}{\mathrm{L_q}} \end{bmatrix}, \mathrm{y} = \mathrm{x} = \begin{bmatrix} \mathrm{i_{ds}} \\ \mathrm{i_{qs}} \end{bmatrix} \tag{15}$$

$$\mathbf{u} = \begin{pmatrix} \mathbf{v_{ds}} \\ \mathbf{v_{qs}} \end{pmatrix} = \begin{pmatrix} \mathbf{r_3(i^*_{ds} - i_{ds})} \\ \mathbf{r_2(i^*_{qs} - i_{qs})} \end{pmatrix} = \begin{pmatrix} \mathbf{r_3(i^*_{ds} - i_{ds})} \\ \mathbf{r_2(r_1(\omega_{ref} - \omega_r^*) - i_{qs})} \end{pmatrix} \tag{16}$$

Where $r_{n\,(\mathrm{n=1,2,3\&4})}$ are the transfer functions of the PI controllers of the speed loop, the *q*- and *d*-axes current loop, and the Y-MRAS, respectively.

$$r_1 = \frac{sk_{p1} + k_{i1}}{s}, r_2 = \frac{sk_{p2} + k_{i2}}{s}, r_3 = \frac{sk_{p3} + k_{i3}}{s}, r_4 = \frac{sk_{p4} + k_{i4}}{s} \tag{17}$$

Using the small-signal analysis with respect to the operating point of x_0, Eqs. 13 and 14 become:

$$\dot{\Delta x} = A\Delta x + \Delta A x_0 + B\Delta u + \Delta E \tag{18}$$

$$\Delta y = C\Delta x \tag{19}$$

Taking the Laplace transformation and substituting Eq. 18 into Eq. 19 gives:

$$\Delta y = C(sI - A)^{-1}[\Delta A x_0 + B\Delta u + \Delta E] \tag{20}$$

Where,

$$\mathbf{x_0} = \begin{pmatrix} \mathbf{i_{ds0}} \\ \mathbf{i_{qs0}} \end{pmatrix}, \Delta\mathbf{u} = \begin{pmatrix} \mathbf{\Delta v_{ds}} \\ \mathbf{\Delta v_{qs}} \end{pmatrix} = \begin{pmatrix} \mathbf{-r_3 \Delta i_{ds}} \\ \mathbf{-r_2 \Delta i_{qs} - r_1 r_2 \Delta w_r)} \end{pmatrix},$$

$$\Delta\mathbf{y} = \begin{pmatrix} \mathbf{\Delta i_{ds}} \\ \mathbf{\Delta i_{qs}} \end{pmatrix}, \ \Delta\mathrm{E} = \begin{pmatrix} 0 \\ \frac{-\Delta\omega_r P \lambda_{af}}{\mathrm{L_q}} \end{pmatrix}, \Delta\mathrm{A} = \begin{bmatrix} 0 & \frac{\mathrm{L_q}}{\mathrm{L_d}} \\ \frac{-\mathrm{L_d}}{\mathrm{L_q}} & 0 \end{bmatrix} \Delta\omega_s \tag{21}$$

Substituting the values of $\boldsymbol{A, B, C, \Delta A, \Delta u, \Delta E}, and\ \boldsymbol{x_0}$ in Eq. 20 generates the expression for $\left(\frac{\Delta i_{qs}}{\Delta \omega_r}\right)$ and $\left(\frac{\Delta i_{ds}}{\Delta \omega_r}\right)$.

From Eq. 9, the error of the rotor-speed estimation is given by:

$$\varepsilon = Y_1 - Y_4 \tag{22}$$

Where $Y_4\ and\ Y_1$ are steady state and instantaneous fictitious quantities. The stability analysis is conducted in the rotor reference frame (of the *d*- and *q*-axes). Both quantities are expressed in the rotating reference frame.

$$\varepsilon = (v_{qs} i_{qs} - v_{ds} i_{ds}) - \left(\mathrm{R}_s i_{qs}^2 + \omega_r^* P i_{qs} \lambda_{af}\right) \tag{23}$$

$$\varepsilon = v_{qs} i_{qs} - v_{ds} i_{ds} - \mathrm{R}_s i_{qs}^2 - \omega_r^* P i_{qs} \lambda_{af}$$

Considering a small perturbation in ε, Δε can be expressed as:

$$\Delta\varepsilon = v_{qs}\Delta i_{qs} - v_{ds}\Delta i_{ds} - 2\mathrm{R}_s i_{qs}\Delta i_{qs} - P i_{qs}\lambda_{af}\Delta\omega_r^* - \omega_r^* P \lambda_{af}\Delta i_{qs} \tag{24}$$

Dividing Eq. 24 by $\Delta\omega_r$ gives:

$$\frac{\Delta\varepsilon}{\Delta\omega_r} = v_{qs}\frac{\Delta i_{qs}}{\Delta\omega_r} - v_{ds}\frac{\Delta i_{ds}}{\Delta\omega_r} - 2R_s i_{qs}\frac{\Delta i_{qs}}{\Delta\omega_r} - Pi_{qs}\lambda_{af}\frac{\Delta\omega_r^*}{\Delta\omega_r} - \omega_r^* P\lambda_{af}\frac{\Delta i_{qs}}{\Delta\omega_r} \quad (25)$$

From the Y-MRAS adaption mechanism from Eq. 8:

$$\Delta\omega_r^* = r_4 * \Delta\varepsilon$$
$$\Delta\varepsilon = \frac{\Delta\omega_r^*}{r_4} \quad (26)$$

Substituting $\Delta\varepsilon$ (i.e., Eq. 26) in Eq. 25 gives:

$$\frac{\Delta\omega_r^*}{r_4\Delta\omega_r} = v_{qs}\frac{\Delta i_{qs}}{\Delta\omega_r} - v_{ds}\frac{\Delta i_{ds}}{\Delta\omega_r} - 2R_s i_{qs}\frac{\Delta i_{qs}}{\Delta\omega_r} - Pi_{qs}\lambda_{af}\frac{\Delta\omega_r^*}{\Delta\omega_r} - \omega_r^* P\lambda_{af}\frac{\Delta i_{qs}}{\Delta\omega_r}$$

$$\frac{\Delta\omega_r^*}{\Delta\omega_r}(1 + r_4 i_{qs} P\lambda_{af}) = r_4\left(v_{qs}\frac{\Delta i_{qs}}{\Delta\omega_r} - v_{ds}\frac{\Delta i_{ds}}{\Delta\omega_r} - (2R_s i_{qs} + \omega_r^* P\lambda_{af})\frac{\Delta i_{qs}}{\Delta\omega_r}\right) \quad (27)$$

Let:

$$G(s) = \left(v_{qs}\frac{\Delta i_{qs}}{\Delta\omega_r} - v_{ds}\frac{\Delta i_{ds}}{\Delta\omega_r} - (2R_s i_{qs} + \omega_r^* P\lambda_{af})\frac{\Delta i_{qs}}{\Delta\omega_r}\right)$$
$$\frac{\Delta\omega_r^*}{\Delta\omega_r}(1 + r_4 i_{qs} P\lambda_{af}) = r_4 G(s) \quad (28)$$

The closed-loop representation of the Y-MRAS-based speed-estimation for the vector-control PMSM drive is shown in Figure 2a from Eq. 29. The closed-loop transfer function is given by:

$$\frac{\Delta\omega_r^*}{\Delta\omega_r} = \frac{G(s) * r_4}{(1 + r_4 i_{qs} P\lambda_{af})} \quad (29)$$

The stability of the PMSM drive was checked for the Y-MRAS speed estimation closed-loop system using Routh–Hurwitz criteria in the speed-to-torque domain with small increments in speed and torque values at several operating points. The system is said to be unstable if any roots of the characteristic equation lie in the right half of the s-plane. The obtained stable and unstable points in the speed–torque domain are plotted in Figure 2b. The green dots represent the stable regions for the MRAS gain.

The stability for various operating points in all four quadrants was verified using MATLAB software. The speed was changed from -200 rad/sec to 200 rad/sec in the form of a ramp command for various fixed loads. The corresponding simulation results are shown in Section V. It is observed that the Y-MRAS speed-estimation technique is completely stable for a wide speed–torque range in all four quadrants. The stability was verified by a small-signal analysis consideration of unit-step variation; this analysis cannot guarantee the stability of large signals as sometimes, the motor goes to transient for a large disturbance.

The Bode plot [41] of Eq. 29 is shown in Figure 2c and 2d; it includes one motoring operating point and one in the regenerating mode. Figure 2c contains the Bode plot for the forward motoring operation (speed: 80 rad/sec with a load of 4.4 Nm). The Bode plot for the regenerating mode (speed: 80 rad/sec with a load of -4.4 Nm) is revealed in Figure 2d. Here, the plot shows both the infinite gain margin and the infinite phase margin, which demonstrates the robustness of the speed-estimation algorithm. All zeros and poles are seen, as presented in the left-half of the s-plane from the root locus [42] shown in Figure 2c and 2d. This confirms the stability of the speed-estimation technique in both motoring and generating modes.

Sensitivity analysis

The sensitivity of the sensorless speed-control technique to variations in stator resistance is studied and presented. The adaptive Y-MRAS model is sensitive to stator-resistance variation. The sensitivity analysis [43] is similar to the stability analysis, except for the linearizing, which is conducted with respect to R_s.

The expression of A with respect to R_s, from Eq. 15:

$$\Delta\mathbf{A} = \begin{bmatrix} \frac{-1}{L_d} & 0 \\ 0 & \frac{-1}{L_q} \end{bmatrix}\Delta R_s \quad (30)$$

Substituting the values of $\boldsymbol{A}, \boldsymbol{B}, \boldsymbol{C}, \Delta\boldsymbol{A}, \Delta\boldsymbol{u}, \Delta\boldsymbol{E}$ and $\boldsymbol{x_0}$ in Eq. 20 generates the expression for $\left(\frac{\Delta i_{qs}}{\Delta R_s}\right)$ and $\left(\frac{\Delta i_{ds}}{\Delta R_s}\right)$.

The $\mathcal{E}$ is linearized with respect to R_s:

$$\Delta\varepsilon = v_{qs}\Delta i_{qs} - v_{ds}\Delta i_{ds} - 2R_s i_{qs}\Delta i_{qs} - i_{qs}^2\Delta R_s - P\lambda_{af}(i_{qs}\Delta\omega_r^* + \omega_r^*\Delta i_{qs}) \quad (31)$$

Dividing Eq. 31 by ΔR_s gives:

$$\frac{\Delta\varepsilon}{\Delta R_s} = v_{qs}\frac{\Delta i_{qs}}{\Delta R_s} - v_{ds}\frac{\Delta i_{ds}}{\Delta R_s} - 2R_s i_{qs}\frac{\Delta i_{qs}}{\Delta R_s} - i_{qs}^2 - P\lambda_{af}\left(i_{qs}\frac{\Delta\omega_r^*}{\Delta R_s} + \omega_r^*\frac{\Delta i_{qs}}{\Delta R_s}\right) \quad (32)$$

From the Y-MRAS adaption mechanism from Eq. 26:

$$\frac{\Delta\omega_r^*}{\Delta R_s}(1 + r_4 i_{qs} P\lambda_{af}) = r_4\left(v_{qs}\frac{\Delta i_{qs}}{\Delta R_s} - v_{ds}\frac{\Delta i_{ds}}{\Delta R_s} - 2R_s i_{qs}\frac{\Delta i_{qs}}{\Delta R_s} - i_{qs}^2 - P\lambda_{af}\omega_r^*\frac{\Delta i_{qs}}{\Delta R_s}\right) \quad (33)$$

Let,

$$H(s) = \left(v_{qs} - 2R_s i_{qs} - P\lambda_{af}\omega_r^*\right)\frac{\Delta i_{qs}}{\Delta R_s} - i_{qs}^2 - v_{ds}\frac{\Delta i_{ds}}{\Delta R_s} \quad (34)$$

$$\frac{\Delta\omega_r^*}{\Delta R_s} = \frac{H(s) * r_4}{(1 + r_4 i_{qs} P\lambda_{af})} \quad (35)$$

The sensitivity of the Y-MRAS with an R_s variation is performed at a rated load; $\left|\frac{\Delta\omega_r^*}{\Delta R_s}\right|$ to ω_r is shown in Figure 3.

Modified YR-MRAS-Based Stator-Resistance-Estimation Technique

This paper proposes a new YR-MRAS for the online resistance-estimation technique. From Eq. 1, the *d*-axis stator voltage of the PMSM assigned to the rotor reference frame can be expressed as:

$$v_{ds} = R_s i_{ds} + L_d\frac{di_{ds}}{dt} - \omega_s L_q i_{qs} \quad (36)$$

In a steady state, the derivative terms are zero, and the new expression for v_{ds} becomes [31]:

$$v_{ds} = R_s i_{ds} - \omega_s L_q i_{qs} \quad (37)$$

From the vector-controlled PMSM drive, ($i_{ds} = 0$) is imposed in Eq. 37. The simplified expression for v_{ds} is:

$$v_{ds} = -\omega_s L_q i_{qs} \quad (38)$$

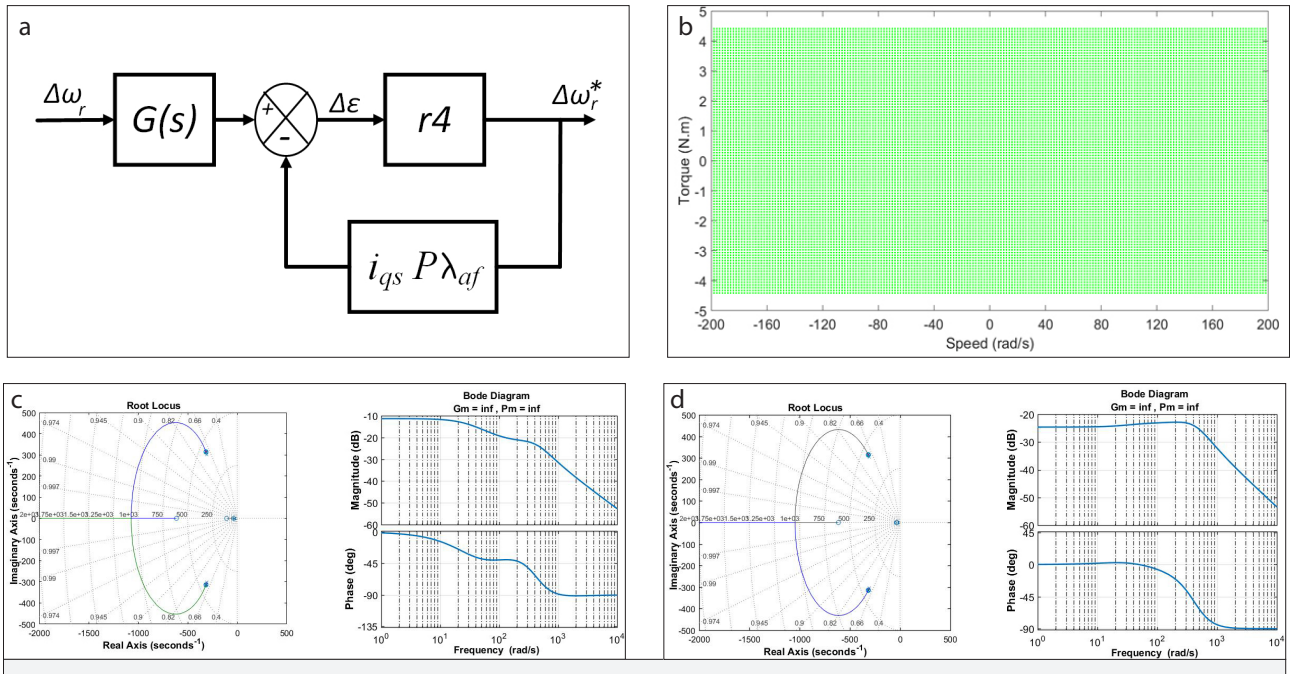

Figure 2. a-d. Closed loop representation of Y-MRAS based speed-estimator (a) Stable points in the speed-torque domain for Y-MRAS (b). Bode plot and root locus of Y-MRAS for speed estimation (c). Motoring Mode, 80 rad/s with 4.4 N.m load (d). Regenerating Mode 80 rad/s with -4.4 N.m load

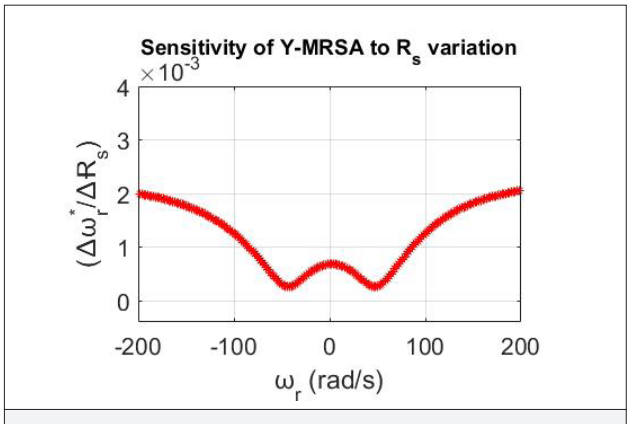

Figure 3. Sensitivity of the Y-MRAS to variations in stator resistance

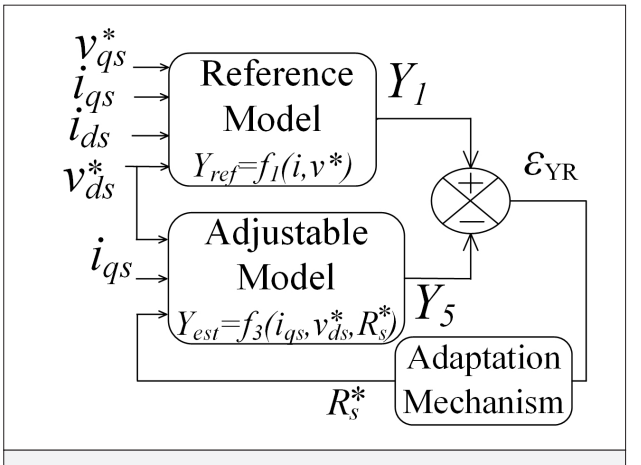

Figure 4. The YR-MRAS-based stator-resistance technique

$$\omega_s i_{qs} = -\frac{v_{ds}}{L_q} \tag{39}$$

Substituting Eq. 39 in Eq. 7 gives:

$$Y_5 = \mathrm{R}_s i_{qs}^2 - \frac{v_{ds}}{L_q}\lambda_{af} \tag{40}$$

$$\varepsilon = (v_{qs}i_{qs} - v_{ds}i_{ds}) - (\mathrm{R}_s^*(\varepsilon,t)i_{qs}^2 - \frac{v_{ds}\lambda_{af}}{L_q}) \tag{41}$$

Above, Eq. 40 is dependent on R_s, L_q and λ_{af} and is free from derivative, integrator, and speed terms. As L_q is constant below the saturation limit, λ_{af} remains constant (with no flux weakening). Y_5 is dependent only on R_s and is independent of speed. Y_1 and Y_5 are considered as reference and adjustable models, respectively. Error (Eq. 41) is evaluated from the difference between Y_1 and Y_5; the error is passed through an adaption mechanism, which is normally a PI controller. The output of the adaption mechanism is the estimated quantity, i.e., the estimated stator resistance (R_s^*), which is used for tuning the adjustable model to reduce the error to zero. This estimated resistance is fed to the speed-estimation technique for R_S compensation. Figure 4 reveals the block diagram of the proposed stator-resistance-estimation technique. The online estimation of R_S gives information about the stator winding temperature from Eq. 42, where $\Delta T, \mathrm{R}_S, \mathrm{R}_0$, and α represent the deviations in temperature, estimated stator resistance, initial stator resis-

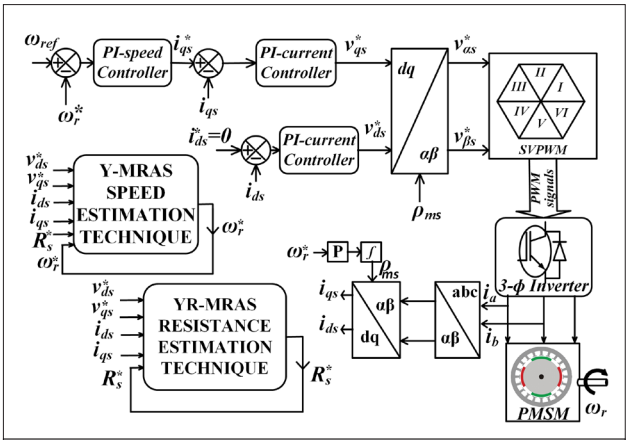

Figure 5. The sensorless speed vector-control PMSM drive

tance, and the temperature coefficient of the stator winding, respectively.

$$\Delta T = (\mathrm{R}_S.\mathrm{R}_o^{-1} - 1)\alpha^{-1} \quad (42)$$

Simulation Results

The proposed Y-MRAS-based speed-estimation technique for a sensorless speed vector-controlled PMSM drive (Figure 5) was verified using software under various operation speeds/loads and is shown below. Two current sensors were used in the drive to measure the balanced three-phase stator currents. The speed loop was closed with the estimated speed, and the position was extracted (Eq. 10) and used in the Clarke and Park frame transformation. The machine parameters were taken from [44] and are shown in Table 1. The proposed technique performs satisfactorily over Q-MRAS [6] at slow zero crossings. The estimated and the actual speed/position overlap, which verifies the robustness of the Y-MRAS speed-estimation technique. The machine currents are shown in the rotor reference frame of the *d*- and *q*-axes. $i_{ds} = 0$ indicates the successful operation of the vector control, and i_{qs} shows the torque-component current. The information for the estimated position is plotted with the actual position in the electrical angle (i.e., in rad), and the position error is shown between the actual and estimated positions. The proper tuning of the PI controller gains improves the system's performance. The shaft speed is at the same scale as the estimated and reference speeds to demonstrate the precision of the Y-MRAS estimation technique.

The drive response for the rated speed with step load

The performance of the drive was verified for no load to full load at rated speeds. The reference speed was changed from 0 rad/sec to 200 rad/sec (from t=0 sec to t=1 sec) under no load. At t=1.5 sec, the machine was fully loaded (i.e., 4.4 Nm) in a step command. At t=2 sec, the speed was changed to 100 rad/sec by a ramp command in 0.5 sec. The load on the machine was changed in a step command to 2.2 Nm and to 4.4 Nm at t=3 and 4 sec, respectively. Figure 6 presents the electrical and load torques on the machine and the machine's shaft speed

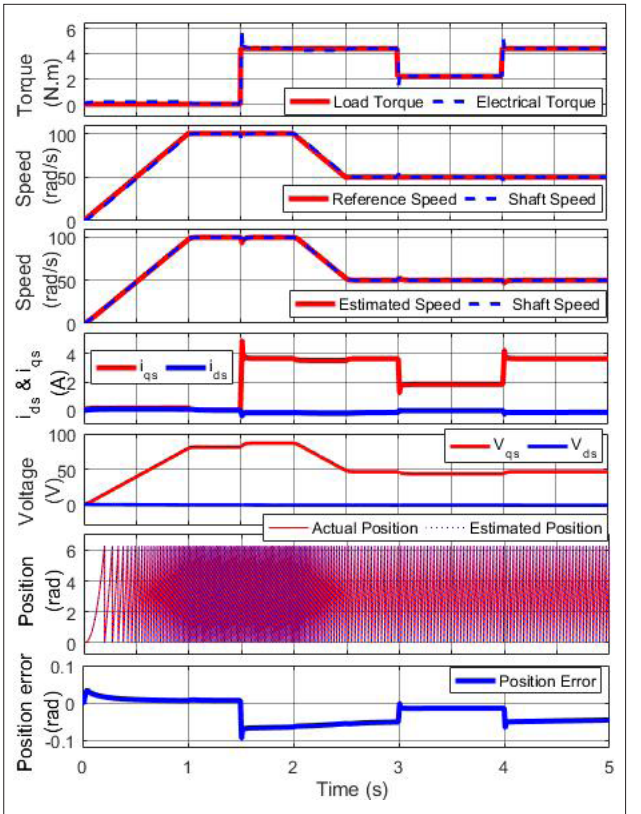

Figure 6. The simulation results for rated speed with a step load

with both reference and estimated speeds. The stator currents and reference voltages are presented in the *d*- and *q*-axes of the rotor reference frame. The actual and estimated positions are presented, and the accuracy of the proposed algorithm is demonstrated by the position error.

The drive response for the ramp-type reference speed

The reference speed was changed in a time-varying ramp profile with constant torque/speed load ($k\omega_r$ *load*). The performance of the sensorless speed PMSM drive was verified for both forward and reverse operating modes. Equation [6] proposes the Q-MRAS speed-estimation technique. It is observed that this technique is problematic at slow to zero speed crossings; however, this is overcome by the proposed Y-MRAS technique. The stator currents are shown in the *d*- and *q*-axes reference frame. i_{ds}=0 shows the vector control of the PMSM drive, and i_{qs} represents the torque-component current. The actual and estimated positions presented in Figure 7 confirm the viability of the proposed speed-estimation technique.

The drive response for the step-type reference speed

Figure 8 contains the forward and reverse motoring information for the PMSM drive with a constant torque/speed load ($k\omega_r$ *load*) for the step speed command. The reference speed was changed in the step commands from 10 rad/sec to −10 rad/sec and back to 10 rad/sec at t=2 sec and t=4 sec; the load on the machine also changed in the step commands,

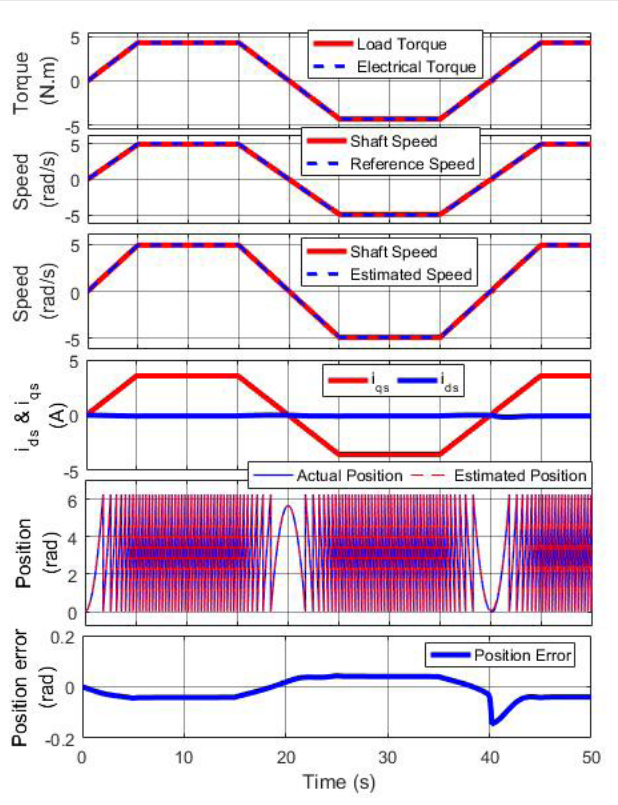

Figure 7. The simulation results for the ramp-type speed command

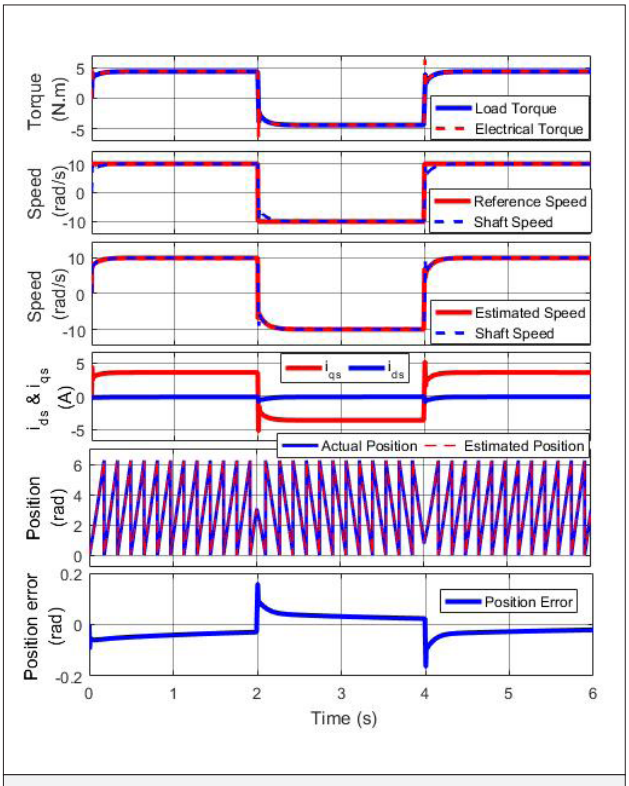

Figure 8. The simulation results for the step-type speed command

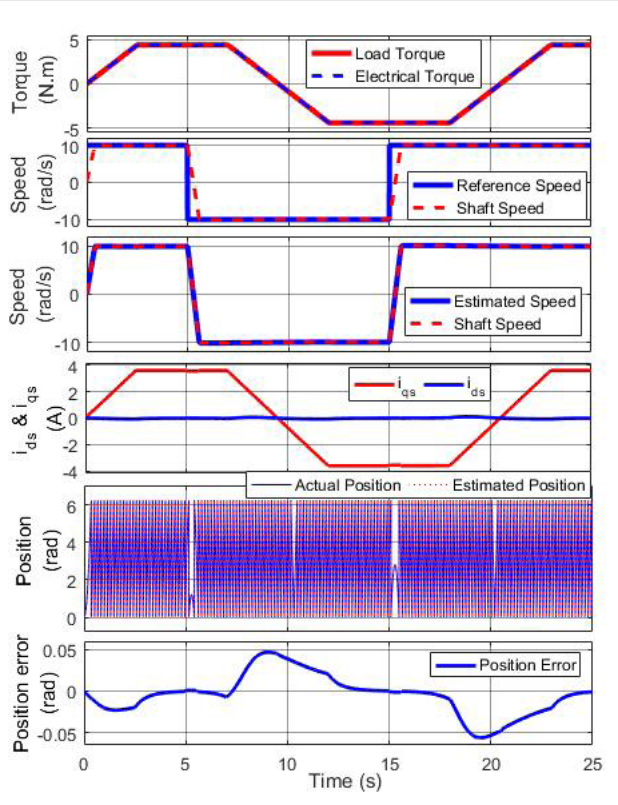

Figure 9. The simulation results for four-quadrant operation

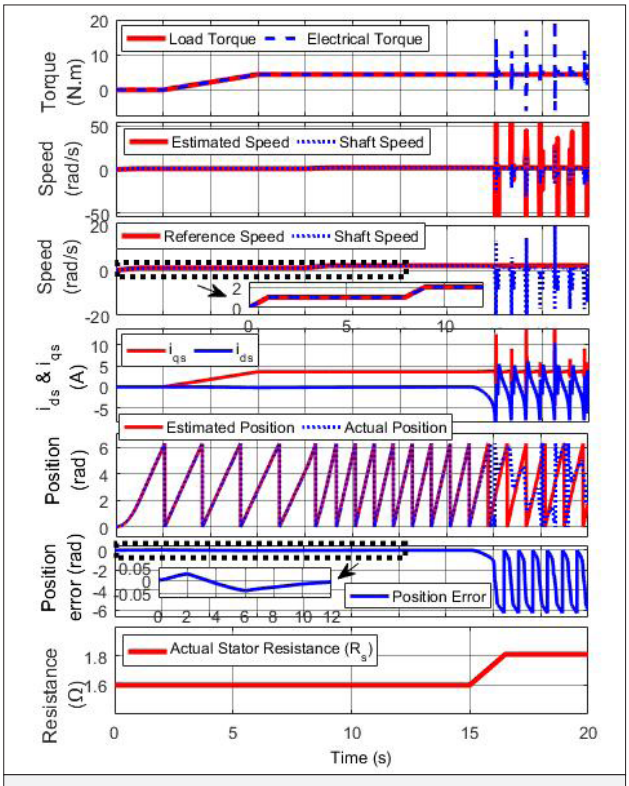

Figure 10. The simulation results for stator-resistance variation at low-speed operation

respectively. Both the shaft position and the position error confirm the accuracy of the proposed speed-estimation technique. The proposed approach was verified for both the ramp and step speed commands from Figure 7 and 8. It is confirmed that the Y-MRAS speed-estimation technique performs satisfactorily at slow zero crossings and for step-speed commands.

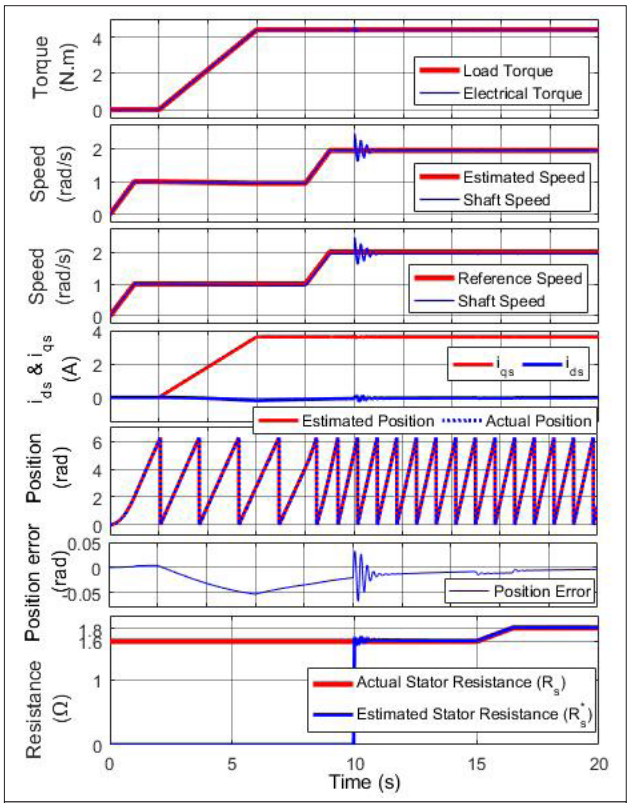

Figure 11. The simulation results with stator-resistance compensation

The drive response for four-quadrant operation

The sensorless speed PMSM drive was verified for four-quadrant operation using step reference speed and slow ramp-load change. The reference speed was changed by step command from 10 rad/sec to −10 rad/sec at 5 sec and was set to 10 rad/sec at t=15 sec. The load was altered in a slow ramp change from 4.4 Nm to -4.4 Nm, as shown in Figure 9. From the speed and load characteristics also presented in the same figure, the forward motoring, reverse regenerating, reverse motoring, forward regenerating, and forward motoring operations are seen at t=0–5 sec, 5–9 sec, 9–15 sec, 15–21 sec, and

Figure 12. Typhoon HIL setup

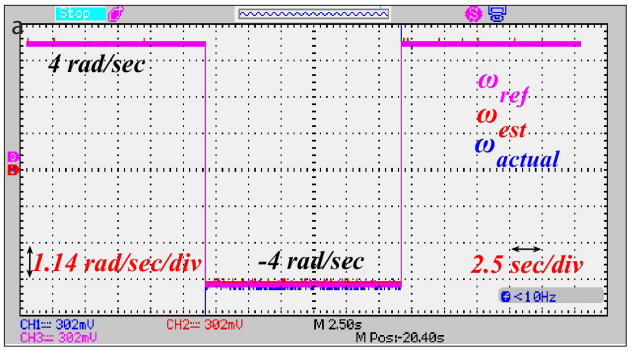

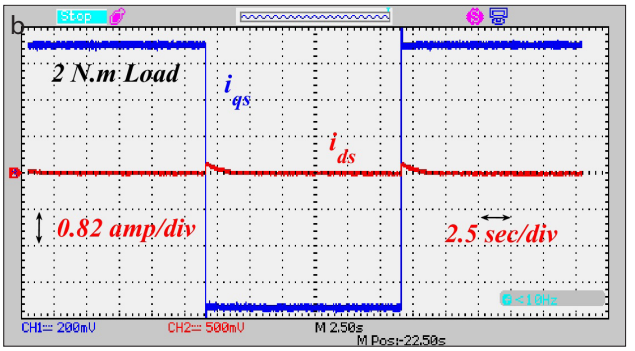

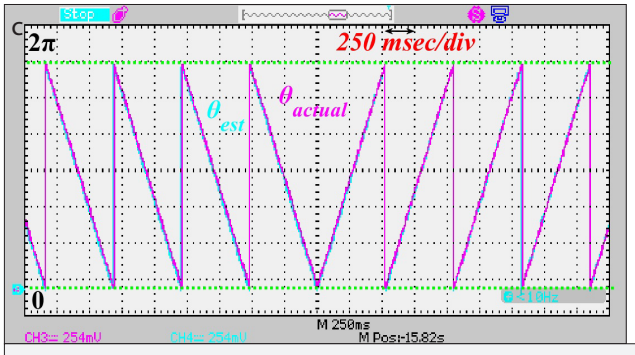

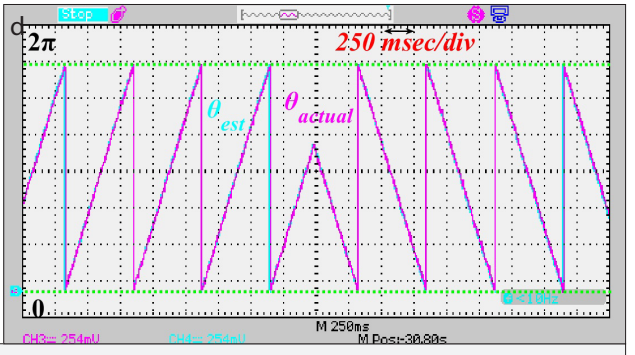

Figure 13 a-d. The Typhoon HIL results for the speed-reversal operation with a step change

21–25 sec, respectively. The actual and estimated positions are shown, and the position error confirms the accuracy of the proposed speed-estimation technique for four-quadrant operation. The dynamics can be overcome by the proper tuning of the PI gains.

The drive response for stator-resistance variation

The variation in stator resistance was observed due to the temperature change of the stator windings. The Y-MRAS speed-estimation technique is dependent on stator resistance; however, the variation of R_s will also degrade the drive's performance. The stator-resistance-variation-simulation results are presented in Figure 10. The machine was started with no load, the reference speed was set to 1 rad/sec and 2 rad/sec in t=0–1 sec and t =–9 sec, respectively, in a ramp form. The machine was loaded to 4.4 Nm in a ramp form from t=2–6 sec. From t=15–16.5 sec, an external resistance was added in series to each phase of the machine at 0.2 ohms (12.5% of R_S). It was observed that the Y-MRAS failed to perform the sensorless speed vector-control PMSM drive. At low to high speeds, the Y-MRAS estimated the speed, but the vector control was lost. Therefore, an online stator-resistance-estimation technique is required to improve the performance of the proposed technique.

1) At very low speeds, the Y-MRAS fails to estimate the speed.

2) For low to high speeds, the vector control fails (i.e., $i_{ds} \neq 0$) under R_S variation.

The drive response with stator-resistance compensation

Figure 11 reveals the simulation result for Figure 10, with online stator-resistance compensation for the vector-control PMSM drive, as shown in Figure 5. At t=10 sec, the R_s estimation technique is closed in a loop to the Y-MRAS speed-estimation technique. Therefore, some dynamics are evident in speed, position error, and i_{ds}. The proposed speed and stator-resistance-estimation technique performs satisfactorily under various speed, load, and stator-resistance variations.

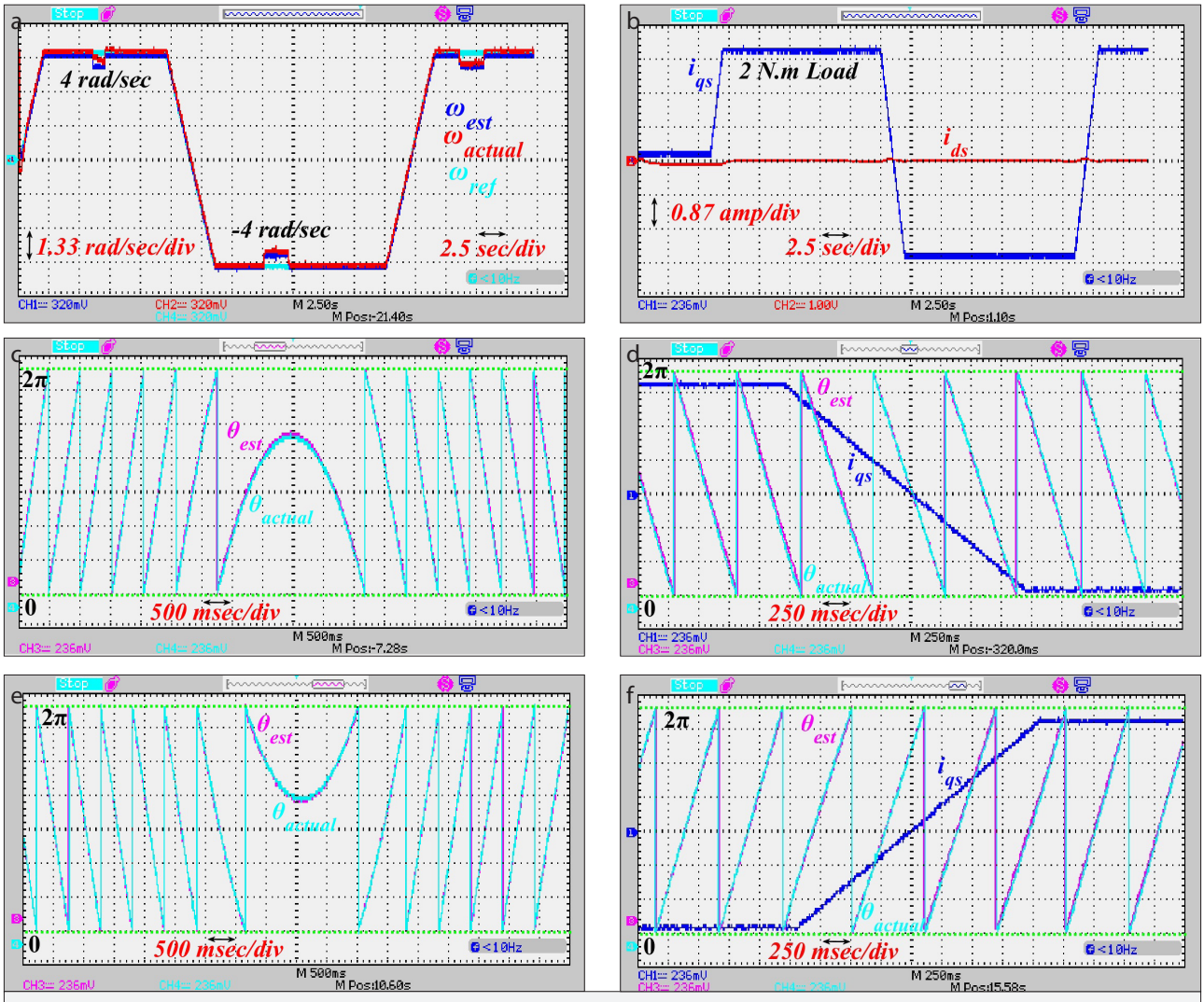

Figure 14 a-f. The Typhoon HIL results for slow zero crossing with four-quadrant operation

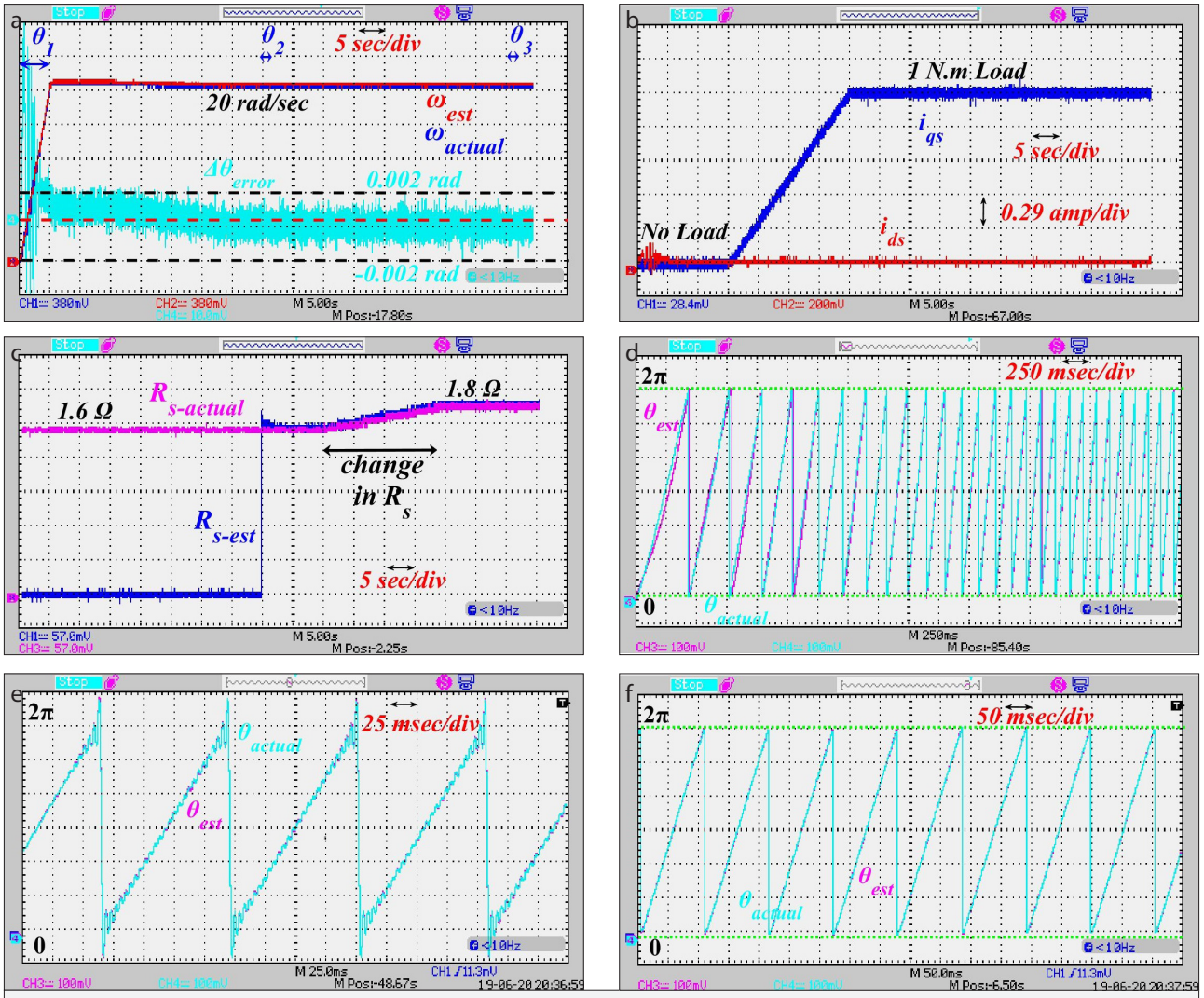

Figure 15 a-f. The HIL results under variations in stator resistance with compensation

Typhoon HIL Real-Time Simulation

An HIL platform was used to verify the proposed speed and the stator-resistance-estimation technique for the vector-control of the PMSM drive. Figure 12 contains the Typhoon hardware in-the-loop (HIL-402) results, and Figure 13-15 show the emulated real-time HIL results for the speed and stator-resistance-estimation techniques.

Typhoon-HIL 402 with 4-processing cores, 32/16-Analog I/O and 32 Digital I/O, and with 16-bit resolution for the most demanding in microgrid, power-quality, motor-drives and controller-test; and verification, and pre-certification tasks is done. It can test in Real-Time with 20 ns PWM-resolution, in closed-loop with high-fidelity power stage with 1 MHz update rate. Moreover, by using the HIL-402 it is possible to simulate the control algorithms with multiple execution-rates and progress the overall-performance of our digitally-simulated HIL system.

The results for the sensorless speed PMSM drive for a step-type speed command with a DC generator-type load are shown in Figure 13. The reference speed was changed from 4 rad/sec to -4 rad/sec at t=15 sec and t=30 sec, respectively. The estimated and actual positions are displayed on the same scale at zero crossings.

Figure 14 contains the four-quadrant operation for the speed-estimation technique for the PMSM drive. The load applied on the machine is represented by i_{qs}, and i_{ds} indicates the drive's vector control. The estimated and actual positions are shown for the zero crossings for speed and load.

Figure 15 reveals the complete speed and stator-resistance-estimation technique for the sensorless speed PMSM drive. The actual and estimated speeds are plotted on the same scale with a position error. The estimated and actual positions are plotted at t=0 sec, t=40 sec, and t=80 sec as θ_1, θ_2, and θ_3, as shown on the speed graph. The estimated stator resistance is

closed in the loop at t=40 sec. The actual and estimated stator resistance is plotted, and the position error is presented with speed to highlight the performance of the drive.

Conclusion

This paper presented a novel technique for estimating stator resistance and rotor speed/position in a vector-controlled PMSM drive. The proposed speed-estimation technique involves stator resistance; any variation in resistance will deteriorate the performance of the drive at low speeds. The proposed technique is applicable for online estimation and compensation and is also suitable for monitoring the stator winding temperature of PMSM machines. The presented approaches are independent of integrator and differentiator terms and are relevant for all PMSM machine types. The Typhoon HIL, the stability and sensitivity analyses, and the MATLAB simulation results all confirm the satisfactory performance of the proposed speed and stator-resistance estimator.

Peer-review: Externally peer-reviewed.

Conflict of Interest: The author have no conflicts of interest to declare.

Financial Disclosure: This work was supported by the Science & Engineering Research Board (FILE NO. ECR/2016/000900), under Early Career Research Award.

References

1. B. K. Bose, "Modern Power Electronics and AC Drives", Prentice Hall PTR, pp. 711, 2002.
2. R. Krishnan, "Permanent Magnet Synchronous and Brushless DC Motor Drives", CRC Press/Taylor & Francis, 2017. [CrossRef]
3. Z. Yan, V. Utkin, "Sliding mode observers for electric machines-an overview", IEEE 2002 28th Annu Conf Ind Electron Soc IECON 02, vol. 3, pp. 1842-7, 2003.
4. G. Zhang, G. Wang, D. Xu, "Saliency-based position sensorless control methods for PMSM drives - A review", Chinese J Electr Eng, vol. 3, no. 2, pp. 14-23, Sep 2019. [CrossRef]
5. P. Borsje, T. F. Chan, Y. K. Wong, S. L. Ho, "A Comparative Study of Kalman Filtering for Sensorless Control of a Permanent-Magnet Synchronous Motor Drive", Electr Mach Drives, pp. 815-22, 2008.
6. S. Maiti, C. Chakraborty, S. Sengupta, "Simulation studies on model reference adaptive controller based speed estimation technique for the vector controlled permanent magnet synchronous motor drive", Simul Model Pract Theory, vol. 17, no. 4, pp. 585-96, Apr, 2009. [CrossRef]
7. B. Sai Shiva, V. Verma, Y. A. Khan, "Q-MRAS-Based Speed Sensorless Permanent Magnet Synchronous Motor Drive with Adaptive Neural Network for Performance Enhancement at Low Speeds", in Innovations in Soft Computing and Information Technology, Singapore: Springer, Singapore, 2019, pp. 103-16. [CrossRef]
8. B. S. Shiva, V. Verma, "Speed and Parameter Estimation of Vector Controlled Permanent Magnet Synchronous Motor Drive", in 2nd International Conference on Energy, Power and Environment: Towards Smart Technology, ICEPE 2018, pp. 1-6. [CrossRef]
9. L. Yongdong, Z. Hao, Li Yongdong, Zhu Hao, "Sensorless Control of Permanent Magnet Synchronous Motor - A Survey", IEEE Veh Power Propuls. Conf, pp. 1-8, Sep, 2008. [CrossRef]
10. T. D. Batzel, K. Y. K. Y. Lee, "An approach to sensorless operation of the permanent-magnet synchronous motor using diagonally recurrent neural networks", IEEE Trans Energy Convers, vol. 18, no. 1, pp. 100-6, Mar, 2003. [CrossRef]
11. D. Xu, B. Wang, G. Zhang, G. Wang, Y. Yu, "A review of sensorless control methods for AC motor drives", Trans Electr Mach Syst, vol. 2, no. 1, pp. 104-15, 2019.
12. A. Khlaief, M. Boussak, A. Châari, "A MRAS-based stator resistance and speed estimation for sensorless vector controlled IPMSM drive", Electr Power Syst Res, vol. 108, pp. 1-15, Marc, 2014. [CrossRef]
13. A. Karthikeyan, K. K. Prabhakaran, C. Nagamani, "Stator flux based MRAS speed and stator resistance estimator for sensorless PMSM drive", in 2017 14th IEEE India Council International Conference, INDICON 2017, 2018. [CrossRef]
14. B. Nahid-Mobarakeh, F. Meibody-Tabar, F. M. F. M. Sargos, "Back EMF estimation-based sensorless control of PMSM: Robustness with respect to measurement errors and inverter irregularities", IEEE Trans Ind Appl, vol. 43, no. 2, pp. 485-94, 2007. [CrossRef]
15. F. Genduso, R. Miceli, C. Rando, G. R. Galluzzo, "Back EMF sensorless-control algorithm for high-dynamic performance PMSM", IEEE Trans Ind Electron, vol. 57, no. 6, pp. 2092-100, Jun, 2010. [CrossRef]
16. D. Raca, P. Garcia, D. D. Reigosa, F. Briz, R. D. Lorenz, "Carrier-signal selection for sensorless control of PM synchronous machines at zero and very low speeds", IEEE Trans Ind Appl, vol. 46, no. 1, pp. 167-78, 2010. [CrossRef]
17. H. Kim, J. Son, J. Lee, Hongryel Kim, Jubum Son, Jangmyung Lee, "A high-speed sliding-mode observer for the sensorless speed control of a PMSM", IEEE Trans Ind Electron, vol. 58, no. 9, pp. 4069-77, Sep, 2011. [CrossRef]
18. Z. Qiao, T. Shi, Y. Wang, Y. Yan, C. Xia, X. He, "New sliding-mode observer for position sensorless control of permanent-magnet synchronous motor", IEEE Trans Ind Electron, vol. 60, no. 2, pp. 710-9, Feb, 2013. [CrossRef]
19. S. Lin, W. Zhang, "An adaptive sliding-mode observer with a tangent function-based PLL structure for position sensorless PMSM drives", Int J Electr Power Energy Syst, vol. 88, pp. 63-74, Jun, 2017. [CrossRef]
20. H. Chaoui, P. Sicard, "Adaptive fuzzy logic control of permanent magnet synchronous machines with nonlinear friction", IEEE Trans Ind Electron, vol. 59, no. 2, pp. 1123-33, 2012. [CrossRef]
21. M. Zolfaghari, S. A. Taher, D. V. Munuz, "Neural network-based sensorless direct power control of permanent magnet synchronous motor", Ain Shams Eng J, vol. 7, no. 2, pp. 729-40, Jun, 2016. [CrossRef]
22. S. Ye, "A novel fuzzy flux sliding-mode observer for the sensorless speed and position tracking of PMSMs", Optik (Stuttg), vol. 171, pp. 319-25, Jun, 2018. [CrossRef]
23. Y. D. Landau, "Adaptive control: The model reference approach", IEEE Trans Syst Man Cybern, vol. SMC-14, no. 1, pp. 169-70, 1984. [CrossRef]
24. V. Verma, C. Chakraborty, "New series of MRAS for speed estimation of vector controlled induction motor drive", in IECON 2014 - 40th Annual Conference of the IEEE Industrial Electronics Society, Dallas, TX, 2014, pp. 755-61. [CrossRef]
25. S. Mohan Krishna, J. L. Febin Daya, "MRAS speed estimator with fuzzy and PI stator resistance adaptation for sensorless induction motor drives using RT-lab", Perspect Sci, vol. 8, pp. 121-6, 2016. [CrossRef]
26. M. Hassan, O. Mahgoub, A. El Shafei, "ANFIS based MRAS speed estimator for sensorless control of PMSM", in 2013 Brazilian Power

Electronics Conference, COBEP 2013 - Proceedings, 2013, pp. 828-35. [CrossRef]
27. S. Fan, W. Luo, J. Zou, G. Zheng, "A hybrid speed sensorless control strategy for PMSM Based on MRAS and Fuzzy Control", Conf Proc - 2012 IEEE 7th Int Power Electron Motion Control Conf - ECCE Asia, IPEMC 2012, vol. 4, pp. 2976-80, 2012.
28. B. S. Shiva, V. Verma, "MRAS Based Speed Sensorless Vector Controlled PMSM Drive", in International Conference on Intelligent Computing, Information and Control Systems (ICICCS), 2020, pp. 549-56. [CrossRef]
29. M. Pulvirenti, G. Scelba, G. Scarcella, M. Cacciato, L. Tornello, "Online stator winding resistance and rotor permanent magnet flux estimation for dual-three phase PMSM drives", Proc IECON 2017 - 43rd Annu Conf IEEE Ind Electron Soc, pp. 2104-9, Jan, 2017. [CrossRef]
30. S. S. Badini, V. Verma, "A New Stator Resistance Estimation Technique for Vector Controlled PMSM Drive", 2018 IEEE Int Conf Power Electron Drives Energy Syst, pp. 1-6, Jul, 2019. [CrossRef]
31. S. Maiti, C. Chakraborty, Y. Hori, M. C. Ta, "Model Reference Adaptive Controller-Based Rotor Resistance and Speed Estimation Techniques for Vector Controlled Induction Motor Drive Utilizing Reactive Power", IEEE Trans Ind Electron, vol. 55, no. 2, pp. 594-601, 2008. [CrossRef]
32. X. Jiang, Z. Zhang, P. Sun, Z. Q. Zhu, "Estimation of Temperature Rise in Stator Winding and Rotor Magnet of PMSM Based on EKF", 3rd Int Conf Comput Electr Eng (ICCEE 2010), vol. 53, pp. 1-7, 2012.
33. B. Nahid-Mobarakeh, F. Meibody-Tabar, F. M. Sargos, "Mechanical sensorless control of PMSM with online estimation of stator resistance", IEEE Trans Ind Appl, vol. 40, no. 2, pp. 457-1, Mar, 2004. [CrossRef]
34. V. R. Nikzad, N. N. Ardekani, A. Dastfan, A. Darabi, "DTC-SVPWM method for PMSM control using a fuzzy stator resistance estimator", ICECT 2011 - 2011 3rd Int Conf Electron Comput Technol, vol. 2, pp. 122-6, 2011. [CrossRef]
35. K. Liu, Z. Q. Zhu, D. A. Stone, "Parameter estimation for condition monitoring of PMSM stator winding and rotor permanent magnets", IEEE Trans Ind Electron, vol. 60, no. 12, pp. 5902-13, 2013. [CrossRef]
36. K. Hartani, M. Sekour, A. Draou, "A new direct torque control scheme for PMSM with on-line stator resistance tuning", Int Conf Power Eng Energy Electr Drives, pp. 721-6, May, 2013. [CrossRef]
37. Y. Xu, U. Vollmer, A. Ebrahimi, N. Parspour, "Online estimation of the stator resistances of a PMSM with consideration of magnetic saturation", EPE 2012 - Proc Int Conf Expo Electr Power Eng, pp. 360-5, 2012.
38. M. Du, Y. Tian, W. Wang, Z. Ouyang, K. Wei, "A Novel Finite-Control-Set Model Predictive Directive Torque Control Strategy of Permanent Magnet Synchronous Motor with Extended Output", Electronics, vol. 8, no. 4, p. 388, Mar, 2019. [CrossRef]
39. V. Verma, C. Chakraborty, S. Maiti, Y. Hori, "Speed Sensorless vector controlled induction motor drive using single current sensor", IEEE Trans Energy Convers, vol. 28, no. 4, pp. 938-50, 2013. [CrossRef]
40. A. V. R. Teja, V. Verma, C. Chakraborty, "A new formulation of reactive-power-based model reference adaptive system for sensorless induction motor drive", IEEE Trans Ind Electron, vol. 62, no. 11, pp. 6797-808, 2015. [CrossRef]
41. R. Kumar, S. Das, A. J. Chattopadhyay, "Comparative assessment of two different model reference adaptive system schemes for speed-sensorless control of induction motor drives", IET Electr Power Appl, vol. 10, no. 2, pp. 141-54, Feb, 2016. [CrossRef]
42. A. Pal, S. Das, "A new sensorless speed estimation strategy for induction motor driven electric vehicle with energy optimization scheme", in 1st IEEE International Conference on Power Electronics, Intelligent Control and Energy Systems, ICPEICES 2016, 2017, pp. 1-6.
43. A. V. Ravi Teja, C. Chakraborty, "A novel model reference adaptive controller for estimation of speed and stator resistance for vector controlled induction motor drives", in 2010 IEEE International Symposium on Industrial Electronics, 2010, pp. 1187-92. [CrossRef]
44. G. R. Gopinath, P. Das Shyama, "Sensorless control of PMSM using an adaptively tuned SCKF", J Eng, pp. 1-5, Jun, 2019. [CrossRef]

Badini Sai Shiva received the B.Tech. degree in electrical and electronics engineering from JNTU Hyderabad, Telangana, India, in 2012 and M. Tech degrees in Energy Systems from JNTUH College of Engineering Hyderabad, Telangana, India in 2015 and in Control Systems from NIT Patna, Bihar, India in 2018. He is currently associated with the Department of Electrical Engineering, National Institute of Technology Patna, India, where he is currently working towards the Ph.D. degree. His research interest includes drives, control, and renewable energy.

Vimlesh Verma was born in Mumbai, India. He received the B.Tech. degree in electrical and electronics engineering from Andhra University, Andhra Pradesh, India, in 2002, M.Tech. degree in power apparatus and systems from Nirma University, Gujarat, India, in 2005 and Ph.D. degree in Electrical Engineering from Indian Institute of Technology Kharagpur, Kharagpur, India in 2015. He is an Assistant Professor in the Department of Electrical Engineering, NIT Patna. His research interests include sensorless control of ac drives, fault diagnosis of induction motor drives, and renewable energy.